University of Tehran Press

Pollution

Print ISSN: 2383-451X
Online ISSN: 2383-4501

https://jpoll.ut.ac.ir/

Fractal Description of the Temporal Fluctuation of PM2.5 and PM10 Concentrations and their Cross-correlation at Cotonou Autonomous Port and the "Boulevard de la Marina" area (Benin Republic, West Africa)

Gabin Koto N'Gobi[1] | Médard Noukpo Agbazo[1,2]✉ | Augustin Leode[1]

1. Laboratoire de Physique du Rayonnement (LPR), Université d'Abomey-Calavi, Abomey-Calavi BP : 526 UAC, Bénin
2. International Chair in Mathematical Physics and Applications (ICMPA-UNESCO Chair), Université d'Abomey-Calavi, Abomey-Calavi BP: 526 UAC, Bénin

Article Info

Article type:
Research Article

Article history:
Received: 2 Sep 2022
Revised: 22 Nov 2022
Accepted: 16 Jan 2023

Keywords:
PM2.5
PM10
Boulevard de la Marina
Cotonou
Pollution levels
Box-counting
Multifractal characteristics
Cross-correlation analysis

ABSTRACT

The present study aims to provide baseline information on the temporal characteristics of PM2.5 and PM10 concentration time series variations, mainly on the cross-correlation between PM2.5 and PM10, using the improved mathematical and nonlinear methods. Firstly, the fractal theory such as fractal dimension is used to detect the pollution level in PM2.5 and PM10 time series. Secondly, the Multifractal Detrending Moving-Average Analysis (MFDMA) is used to analyze the multifractal characteristics of PM2.5 and PM10 concentrations. Thirdly, Multifractal Detrending Moving-Average cross-correlation Analysis (MFXDMA) is used to study the cross-correlation between PM2.5 and PM10 concentrations measured from January 1 to December 31, 2020, along the Boulevard de la Marina, one of the major roads in Cotonou. The results have indicated that: (1) PM10 and PM2.5 concentration time series are characterized by a fractal dimension, which can permit to detect the pollution levels and to analyze the differences in emissions sources; (2) there is a significant multifractal structure in the PM2.5 and PM10 concentration data and their fluctuations are long-range correlated, however, the multifractal properties and self-memory characteristics change with the months; (3) generally, the multifractal degree and the complexity of PM10 are much stronger than those of PM2.5. However, they present a similar multifractality degree in some months of the year; (4) except, in February, the cross-correlation between PM2.5 and PM10 time series in the months of the year presents multifractal characteristics with positive persistence; (5) the cross-correlation multifractal features show monthly variation. This paper provides the inter-relationship between air PM2.5 and PM10 time series which may help taking steps in controlling the air quality and management of the Cotonou port area environment.

Cite this article: Koto N'Gobi, G., Agbazo, Noukpo M., & Leode, A. (2023). Fractal Description of the Temporal Fluctuation of PM2.5 and PM10 Concentrations and Their Cross-correlation at Cotonou Autonomous Port and the "Boulevard de la Marina" area (Benin Republic, West Africa). *Pollution* , 9 (2), 628-645.
http://10.22059/POLL.2022.347740.1608

© The Author(s). Publisher: University of Tehran Press.
DOI: http://10.22059/POLL.2022.347740.1608

INTRODUCTION

Although: (1) air pollution by particulate matter is recognized globally as one of the most concerning environmental problems because of its significant negative impacts on human and ecological health and on national development (WHO, 2016, 2018, 2020), (2) the particulate

*Corresponding Author Email: *agbazomedard@yahoo.fr*

matter such as PM2.5 and PM10 with a respectively aerodynamic diameter smaller than 2.5 and 10 micrometers are major air pollutants (WHO, 2016) in the Benin Republic, data on PM2.5 and PM10 concentrations are not widely measured and are unavailable over a long period. This lack of data related to PMs constitutes a limitation to the understanding of several aspects of air pollution and especially in their modeling process in the Benin Republic (Awokola et al., 2020). To overcome this unavailability of data, during the international research program named DACCIWA (Dynamic Aerosol-Cloud-Chemistry Interaction in West Africa), weekly-scale mass concentrations of PM2.5 and PM10 were measured from February 2015 to March 2017 in Cotonou (Benin) and Abidjan (Côte d'Ivoire) (Knippertz et al., 2015; Evans et al., 2018). These data allowed Djossou et al.(2018) to study the level of air pollution in these two cities and to produce the first contribution to aerosol source identification within the two cities. They showed that in Cotonou, the concentration of PM2.5 is three times greater than the standard recommended by the World Health Organization. The authors found severe air pollution in Cotonou and Abidjan. But, the temporal resolution of the data measured during the DACCIWA program is prohibitive for studies on the variation of PM2.5 and PM10 concentrations on fine temporal scales. Recently, during the Beninese-German scientific mission financed by the German Corporation for International Cooperation GmbH (GIZ), PM10, PM4, PM2.5, and PM1 mass concentration, and meteorological variables at a 15-minutes scale were measured in Cotonou, along the Boulevard de la Marina, a major road in Cotonou (Kounouhewa et al., 2020). Based on the data measured during January 2020 by this international cooperation, Kounouhewa et al. (2020) confirmed Djossou's work, and have shown that the concentration of PM2.5 and PM10 are greater than the WHO recommendation in terms of concentration.

Moreover, during the collaborative research project between Lancaster University, the Liverpool School of Tropical Medicine and the Measuring Air Quality for Advocacy in Africa (MA3) initiative of the African Center for Clean Air (ACCA), Awokola et al. (2020) have evaluated the feasibility and practicality of longitudinal measurements of ambient PM2.5 using low-cost air quality sensors (Purple Air-II-SD) across thirteen locations in seven countries in sub-Saharan Africa, such as Benin Republic (Cotonou), Burkina Faso (Ouagadougou), Gambia (Fajara), Nigeria (Lagos, Enugu, Anambra), Cameroon (Douala), Kenya (Nairobi), Uganda (Kampala). Using the PM2.5 concentration data collected continuously from January 1st to December 31st 2019, they have indicated high concentrations of PM2.5 at Cotonou.

It is well known and argued by (Mayer,1999; and Kinney, 2008) that environmental pollution is the result of many physical and chemical interactions between anthropogenic and natural conditions; thus, it is a complex system. According to (Xepapadeas,1992; Liu et al., 2003; Esposito et al., 2016) a better understanding of the structure of air pollutant concentrations time series and the dynamic mechanisms that govern their temporal variability are important and needed to strongly improve air pollution prevention policies.

Several authors, for example, Nikolopoulos et al. (2021) have shown that the fractal approach is one of the efficient tools to study the dynamic characteristics of air pollutant concentrations and characterize their temporal structure and variability. This approach was applied by (Wang et al., 2000; Lee et al., 2002, 2003a, 2003b; Ho et al., 2004; Shi et al., 2008, 2015; Ski et al., 2015; Xue et al., 2015; Liu et al., 2015; Zhang et al., 2016, 2019; Goa et al., 2019, and Nikolopoulos et al., 2019, 2021). These authors have demonstrated that nonlinear approaches are required to investigate the complex behavior in air pollutant time series.

To date, in the Benin Republic, limited studies are focused on the analysis of PMs concentration, and the state of art on air pollution is mainly focused on (i) the identification of air pollutants sources, (ii) the investigation of their elemental composition, and (iii) the comparison of the limit of the particulate matter's concentration to those of the WHO and EU recommendation. However, no research study has been focused on a better understanding of PM2.5 and PM10 concentration time series variations, mainly on the cross-correlation between

PM2.5 and PM10 observed around the Cotonou Autonomous Port area and Boulevard de la Marina in Benin by nonlinear approaches.

This study aims to complete the study of Kounouhewa et al. (2020), and to provide baseline information for the understanding of the temporal structure and variabilities of PM2.5 and PM10 concentrations series, especially to characterize the level of air pollution and the cross-correlation properties between PM2.5 and PM10 in the Cotonou port area by the fractal approach.

The remaining contents of the paper are structured as follows: in section 2, study sites, the dataset, and methods are described. Analysis of results and their interpretations are provided in section 3. Finally, the paper is concluded with a summary, key limitations of the study, and outlook for further research in Section 4.

MATERIALS AND METHODS

The Benin Republic is one of the countries in South West Africa, located between, the Republic of Togo and the Federal Republic of Nigeria respectively in the West and the East part of the country. Benin is also boarded in the North and the North-West by the Niger Republic and Burkina Faso, respectively. In the South part, a coastline of around 121 km long (in the Gulf of Guinea) separates the country from the Atlantic Ocean. Cotonou is one of the most populous cities because of its high urban transport of thousands of two-wheeled motorcycle taxis (locally known as « zémidjan »), rejecting smoke fine particles in the atmosphere (Mama et al., 2013). The study site (6.35 N 2.41 E) is located on the border of the main road along the area of Cotonou port in Marina Avenue (Figure 1). The place is a traffic site, representative of anthropogenic emissions from cars, trucks, and two-stroke motorcycles (Kounouhewa et al., 2020). The study area is characterized by four seasons. The long rainy season extends from April to July and the short rainy season from October to November (Agbazo et al., 2019). These two seasons are interspersed with two dry periods that are extended from December to March and from August to September (Dossou, and Glehouenou-Dossou, 2007; Agbazo et al., 2019). March is the hottest month (~30°C), while August is the coldest month (~24°C). Figure 1 below shows the map of the location of the measurement site in Cotonou.

In the present study, air particulate matter data (PM2.5, PM10) was collected from the installed meteorological site in Cotonou (6.35 N, 2.41 E) during the Beninese-German scientific mission (Kounouhewa et al., 2020) from January 1^{rst}, 2020 to December 31st, 2020. The measurement process is previously described in (Kounouhewa et al., 2020). The temporal resolution of the data recording is 15min. The reasons behind the choice of the site are: (i) its proximity to the port area where intense traffic activity is observed, (ii) several types of anthropogenic emissions from cars, trucks, and, two-stroke motorcycles can also be frequently released, (iii) along the Marina Avenue, an intense social life is regularly observed and particulate matter data may be very useful to estimate inhalation exposure to PM 2.5 and PM10.

Different technics are used to reach the objectives of our study. These technics are described below.

(1) The rate of change (ROC) on the PM2.5/PM10 ratio is introduced to reflect the degree of change in the PM2.5/PM10 ratio. According to Zhao et al. (2019), ROC is calculated as follows:

$$ROC = \frac{[(PM2.5/PM10)_{t+1} - (PM2.5/PM10)_t]}{(PM2.5/PM10)_t} \quad (1)$$

Where $(PM2.5/PM10)_{t+1}$ and $(PM2.5/PM10)_t$ are respectively the ratio at time *t+1* and *t*.

(2) The box-counting method developed in (Mandelbrot, 1982; Lovejoy et al., 1987; Hubert

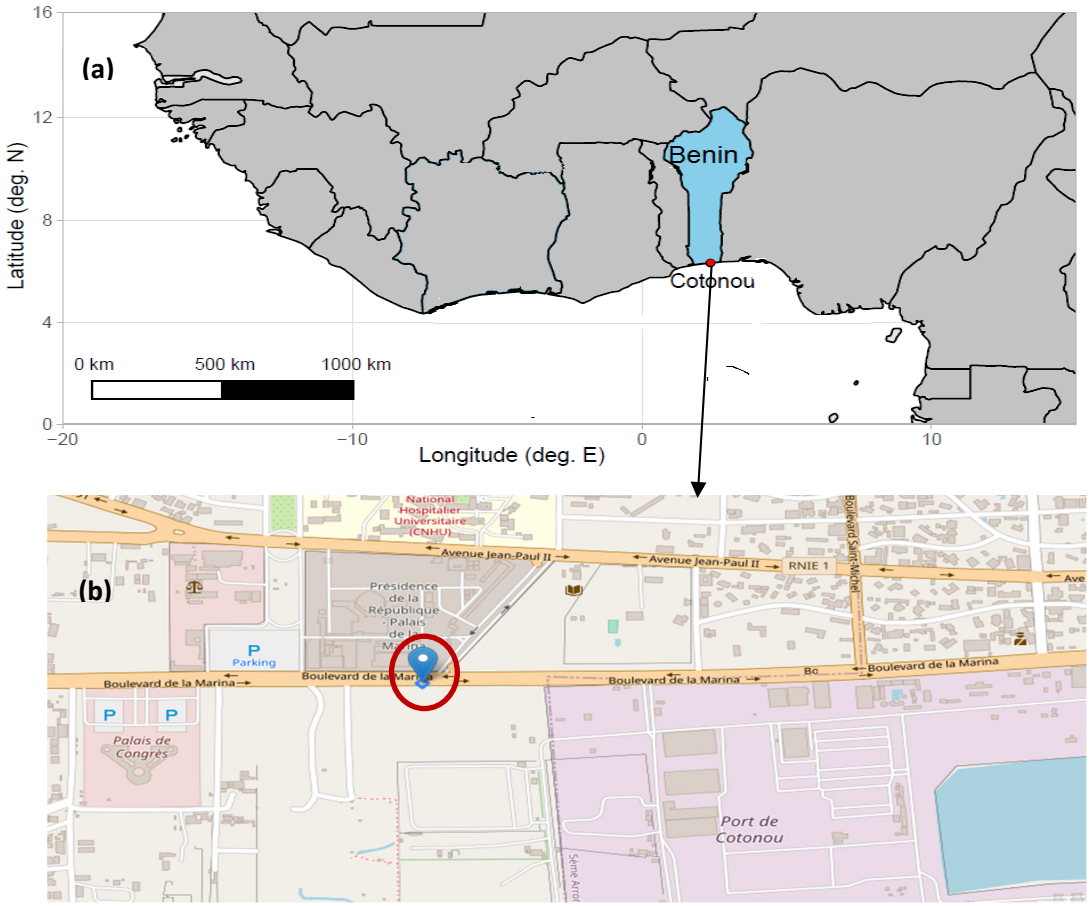

Fig. 1. Geographical location of the study site in Cotonou: (a) Benin location in West Africa and Cotonou city's location in Benin (b) Measurement site's location along Marina Avenue in Cotonou.

and Carbonnel, 1989; Biaou, 2004) is used to compute the fractal dimension (D_f). The calculation process is described as follows:

$$N(\lambda) \propto \lambda^{-D_f} \Rightarrow \log N(\lambda) = -D_f \log(\lambda) + K \tag{2}$$

Where $N(\lambda)$ is the total number of occupied intervals (boxes), in which at least one PM2.5 or PM10 concentration event exceeding the pollution level threshold, *Th*. The threshold is chosen as the WHO recommendation limit for PM2.5 or PM10 concentrations. λ is the length of intervals (boxes), taken as successive powers of 2 $\{2^0, 2^1, 2^2, \ldots\}$. K is a constant. D_f is estimated in the log-log plot as the opposite of the slope. To detect the pollution levels, analyze the emissions sources, and examine the temporal structures of PM2.5 and PM10 concentrations, different pollution levels, *Th* are used: $\{0, 0.5, 1, 1.5, 2, 2.5, 3, 3.5, 4, 4.5\}$ * WHO-limit. WHO-limit is the WHO recommendation for the corresponding particulate matter. According to the World Health Organization (WHO, 2016) standards for daily levels, the WHO limit is $25 \mu g.m^{-3}$ for PM2.5 and $50 \mu g.m^{-3}$ for PM10.

(3) To understand qualitatively and quantitatively the complex behavior of PM2.5 and PM10 concentration, multifractal detrending moving average analysis (MFDMA) developed by Gu and Zhou (2010) is applied. Multifractal detrending moving-average cross-correlation analysis (MFXDMA) developed by Jiang and Zhou (2011) has been applied for the multifractal

characterization of the cross-correlation between the daily PM2.5 and PM10 concentration and the multifractal properties between them**.** The MFXDMA method is decomposed in the following steps:

The first step is to calculate the profiles within the ν^{th} box $[l_\nu + 1, l_\nu + s]$ where $l_\nu = (\nu - 1)s$ of two times series:

$$X_i(k) = \sum_{j=1}^{k} x(l_i + j) \text{ and } Y_i(k) = \sum_{j=1}^{k} y(l_i + j) \quad (3)$$

Where X and Y are respectively the PM2.5 and PM10 concentration time series. The Ms = [M/s] are the non-overlapping boxes of size s that cover each time series and M is the length of the PM2.5 and PM10 concentration time series and *k=1, 2, ..., s*.

The second step is to calculate the cross-correlation for each box as follows:

$$F_i(s) = \frac{1}{s}\sum_{k=1}^{s}[X_i(k) - \tilde{X}_i(k)]\,[\,Y_i(k) - \tilde{Y}_i(k)] \quad (4)$$

Where $\{\tilde{X}_i(k)\}$ and $\{\tilde{Y}_i(k)\}$ are respectively the local trending functions of $\{X_i(k)\}$ and $\{Y_i(k)\}$. The local moving average is adopted as the trend function. According to (Xue et al., 2005; Arianos and Carbone, 2007), the moving average function $\tilde{Z}(t)$ of $Z \in \{X, Y\}$ in a moving window can be calculated as follows:

$$\tilde{Z}(t) = \frac{1}{n}\sum_{k=-\lfloor(n-1)\theta\rfloor}^{\lceil(n-1)(1-\theta)\rceil} Z(t-k) \quad (5)$$

Where *n* is the window size, θ is the position parameter, and it varies in the range [0, 1]. According to Jiang and Zhou (2011), the centered MFXDMA algorithm ($\theta = 0.5$) performs better than the backward and forward MFXDMA algorithms ($\theta = 0$ and $\theta = 1$). Therefore, in the present study, the centered MFXDMA algorithm is adopted.

The third step is to calculate the q^{nth} order cross-correlation as follows:

$$F_{xy}(q,s) = \begin{cases} \left\{\frac{1}{m}\sum_{\nu=1}^{m}\left|F_\nu(s)\right|^{q/2}\right\}^{1/q} & pour\ q \neq 0 \\ exp\left\{\frac{1}{2m}\sum_{\nu=1}^{m} ln\left|F_\nu(s)\right|\right\} & pour\ q = 0 \end{cases} \quad (6)$$

Thus, the following scaling relation is expected when the two series present multifractal nature as:

$$F_{xy}(q,s) \sim s^{h_{xy}(q)} \quad (7)$$

$h_{xy}(q)$ is the q^{nth}-order cross-correlation exponent or the generalized cross-correlation exponent. According to (Zhou, 2008; Jiang and Zhou, 2011; Xu et al., 2017), for nonstationary time series $h_{xy}(q=2) > 1$ and the Hurst exponent is $H = h_{xy}(q=2) - 1$, whereas, for stationary time series, Hurst exponent is $H = h_{xy}(q=2)$. H(2) > 0.5 indicates long memory (positive long-

range) or persistency in the signal and H(2) < 0.5 short memory or anti-persistency. *H(2) = 0.5*, the signal is uncorrelated i.e. white noise. In the case of cross-correlation analysis, $h_{xy}(2)$, is smaller (greater) than 0.5, indicating that there are anti-persistent (persistent) cross-correlations between the PM2.5 and PM10 concentration time series. Anti-persistent behavior implies that a decrease (or increase) of PM2.5 fluctuations is related to an increase (or decrease) of PM10 fluctuations according to power-law. Whereas, the persistent behavior implies that a decrease (or increase) of PM2.5 fluctuations is related to a decrease (or increase) of PM10 fluctuations according to power-law. According to (Xue et al., 2005; Movahed et al., 2006; Arianos and Carbone, 2007; Zhou, 2008; Jiang and Zhou, 2011; Xu et al., 2017), the Renyi exponent $\tau_{xy}(q)$ or the multifractal quality exponent is related to the q[th]-order cross-correlation exponent $h_{xy}(q)$ by the following expression:

$$\tau_{xy}(q) = qh_{xy}(q) - 1 \tag{8}$$

According to (Feder, 1988; Peitgen et al., 2004; Mohaved et al., 2006; Zhou, 2008), the multifractal spectrum $f_{xy}(\alpha_{xy})$ and singularity strengths or the scaling exponent, α_{xy} are related to the q^{th}-order cross-correlation exponent $h_{xy}(q)$ through Legendre transformation as follows:

$$\alpha_{xy} = h_{xy}(q) + qh'_{xy}(q) \tag{9}$$

And

$$f_{xy}(\alpha_{xy}) = q(\alpha_{xy} - h_{xy}(q)) + 1 \tag{10}$$

Some pertinent parameters can be deduced from the multifractal spectrum, they are following:
Multifractal spectrum width, $\Delta\alpha$

$$\Delta\alpha_{xy} = \alpha_{xymax} - \alpha_{xymin} \tag{11}$$

The Holder's exponent, α_{xy0} is defined as the value of α_{xy} at which the multifractal spectrum reaches the maximum value.

The asymmetric index, AI is expressed as:

$$AI = \frac{\Delta\alpha_{xyLeft} - \Delta\alpha_{xyRight}}{\Delta\alpha_{xyLeft} + \Delta\alpha_{xyRight}} \tag{12}$$

Where $\Delta\alpha_{xyLeft} = \alpha_{xy0} - \alpha_{xymin}$ and $\Delta\alpha_{xyRight} = \alpha_{xymax} - \alpha_{xy0}$

These three parameters are used for the quantitative description of PM2.5 and PM10 concentration time series separately and the cross-correlation between them. The asymmetry index (AI) is used to quantify the symmetry of the multifractal spectrum. Also, the AI values explain how the multifractal spectrum is influenced by large- and small-scale fluctuations. AI=0 corresponds to a symmetric shape, $AI > 0$ indicates the right-skewed shape, the multifractal spectrum is caused by small-scale fluctuations, and $AI < 0$ means the left-skewed shape, the time series are characterized by a multifractal structure, which is insensitive to local fluctuations with small amplitudes (Agbazo et al., 2021).

The width of the multifractal spectrum, $\Delta\alpha_{xy}$ is used to characterize the degree of multifractality. Higher values of $\Delta\alpha_{xy}$ correspond to higher multifractal degree and vice versa.

For pure monofractal, $\Delta\alpha_{xy}$ is equal to 0 or less than 0.05 (Makowiec and Fulinski, 2010). α_{xy0} gives valuable information about the structure of the studied process.

According to Gu and Zhou (2010), when $X = Y$, MFXDMA is reduced to MFDMA. Which is used to examine the multifractal characteristics of studied variables.

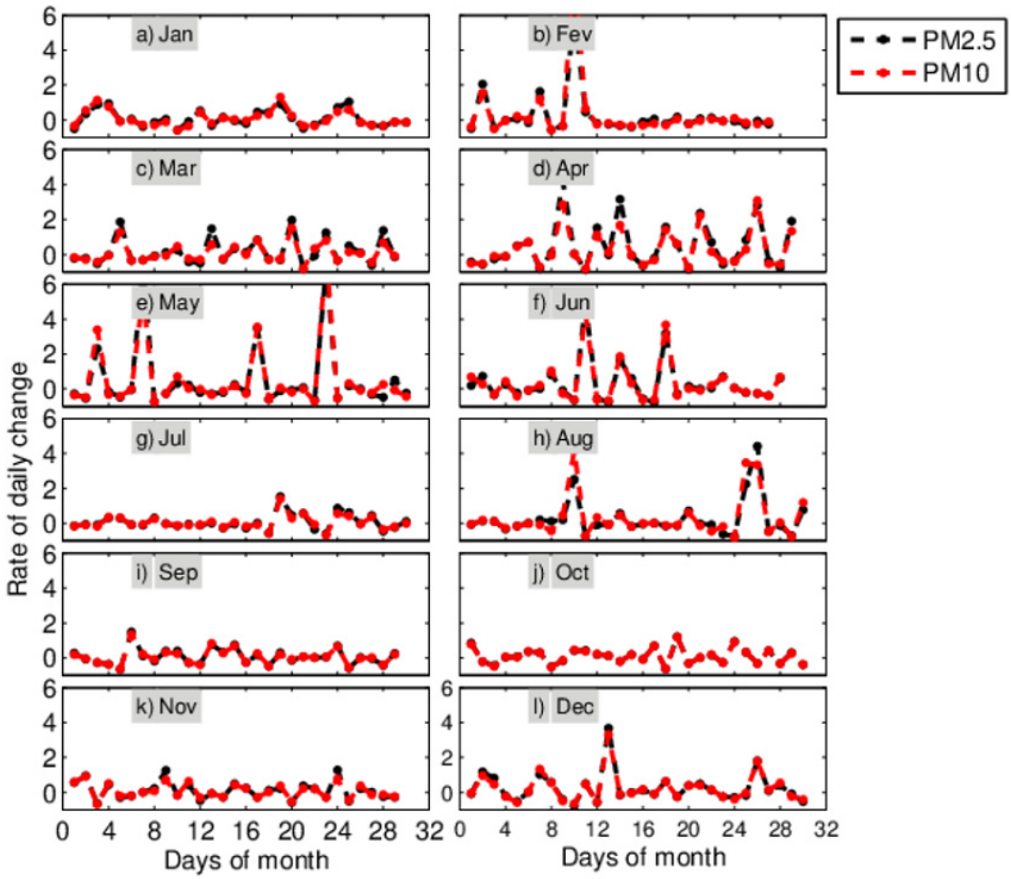

Fig. 2. Temporal variations of ROC on daily particulate matter concentrations in each month. Black color for (PM2.5) and red color (for PM10).

RESULTS AND DISCUSSION

The temporal variation of the Rate of Change (ROC) on PM2.5 and PM10 in each month is shown in Figure 2. From this figure, generally, it's observed that the ROC of PM2.5 is slightly closer to those of PM10, thus they present approximately the same degree of change. This result could be explained by similar sources. For both particulate matters, results show that the ROC varies across days, and sometimes large variability can be observed in some months, such as March, April, May, June, August, and December. These findings indicate that generally the PM2.5 and PM10 concentrations vary substantially from one day to another, and the degree of its change depends on the month. To understand the temporal variation of the pollution level, it is pertinent to analyze the degree of change in the PM2.5/PM10 ratio.

Figure 3 shows the temporal variation of ROC in PM2.5/PM10 concentration ratios. Results show large variability across days in some months and significant differences are found between the months. Considering all the months of the year, the lowest ROC of the PM2.5/PM10 ratio

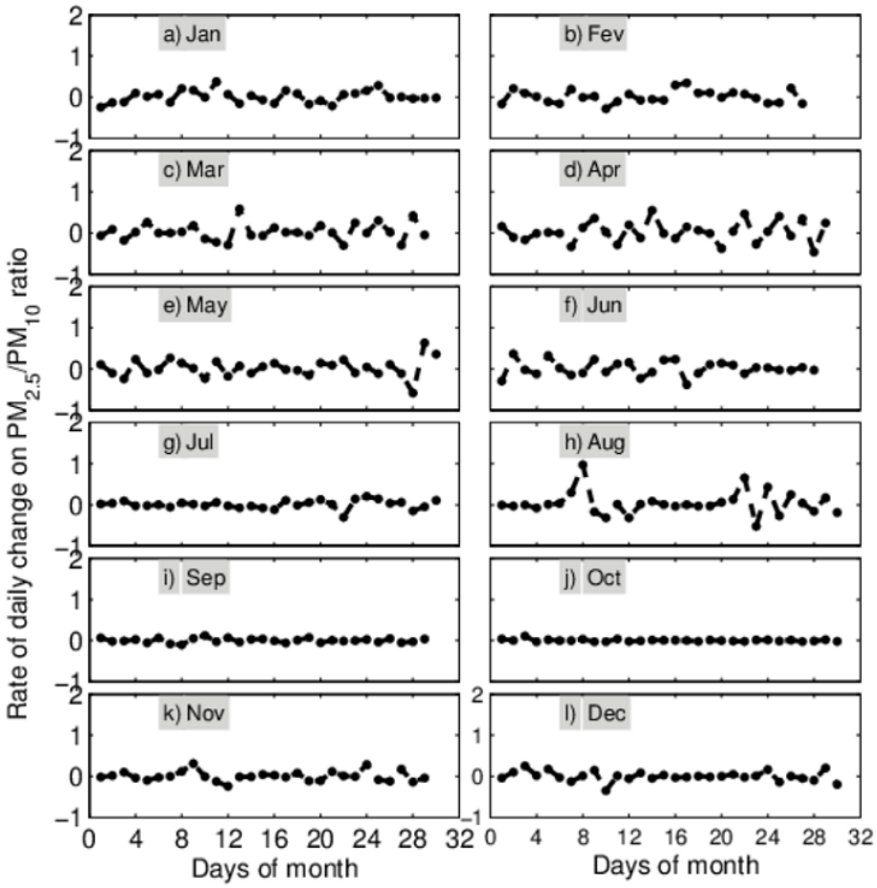

Fig. 3. Temporal variations of ROC on PM2.5/PM10 ratio in each month.

is observed in September and October, which are closer to zero. In July, September, October, November, and December, the ROC doesn't change significantly. This result suggests that in these months PM2.5/PM10 ratios have fewer changes and are stable. These findings indicate the presence of a few sources with low emissions. However, in the other months, the ROC changed significantly, suggesting greater changes in PM2.5/PM10 ratios, and the presence of a relatively unstable proportion of PM2.5. This finding indicates more diversity and variability of emission sources in these months.

Figure 4 shows the number of values per 2D bin for PM10 concentration, and PM2.5 concentration, per month. According to the World Health Organization (WHO), the 24'-h average concentration limits of PM2.5 and PM10 for good air quality are 25 and 50 μg/m^3, respectively. The results demonstrated that from March to December, PM2.5 and PM10 concentrations appear preferentially respectively within the interval (0.0, 25) μg/m^3 and (0.0, 50) μg/m^3. Therefore, in these months, most PM2.5 and PM10 daily concentrations are smaller than or closer to the WHO recommendations. Whereas in January and February PM2.5 and PM10 concentrations appear preferentially respectively within the interval (0.0, 50) μg/m^3 and (0.0, 100) μg/m^3. Thus, most PM2.5 and PM10 daily concentrations are higher than the WHO recommendations in these two months. Overall, the predominance of PM2.5 and PM10 concentrations between respectively 0 and 50 μg/m^3 and 0 and 100 μg/m^3 is identified. However, sometimes, there is a possibility that the PM 2.5 and PM10 concentration becomes respectively higher than 50 μg/m^3 and 100 μg/m^3. The findings indicate that the level of air pollution caused by PM2.5 and PM10 depends on the month. Moreover, there exist some days for which the PM2.5 and PM10 concentrations are much higher than WHO recommendations. These days

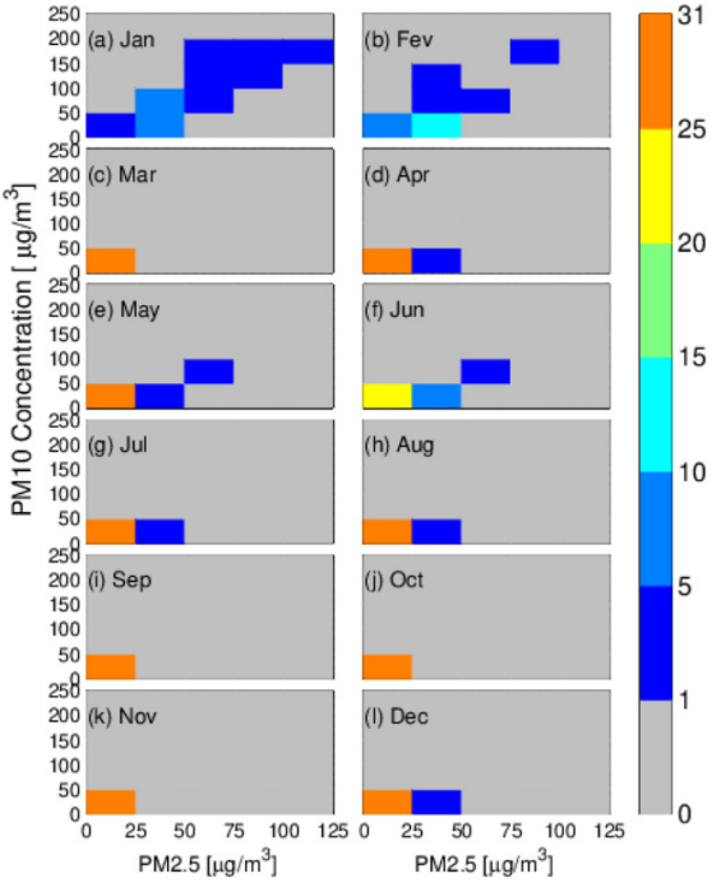

Fig. 4. The number of values per two-dimensional bin (25 µg/m3 × 50µg/m3) of PM10 and PM2.5 concentration, per month.

can appear in all the months but preferentially in the months of the dry season. The total number can exceed 50 (fifty) days in the year.

Figure 5 displays the box-counting results of PM10 and PM2.5 concentrations by using different pollution levels thresholds, *th*. As shown in the figure, (i) the number of boxes N(λ) is a decreasing function of *λ*; (ii) the log-log plots of *N(λ)* versus *λ* present a linear relationship with the slope equal to -1 when *Th* is 0, (iii) with increasing *Th* levels, the log-log plots can be approximate to a straight line with slope different from-1, which represent the opposite of the fractal dimension (*-Df*). These findings indicate that the examined PM10 and PM2.5 concentration time series are characterized by a fractal dimension. Therefore, this approach can be used to identify the scale invariance within a specific time scale range when characterizing the pollution level in particulate matter concentration time series.

Figure 6 describes the relationship between the fractal dimension *(Df)* and the threshold (*Th*) for PM10 and PM2.5 concentrations time series. For both examined PM concentration time series, the fractal dimension decreases with the threshold level. This result suggests that the examined PM2.5 and PM10 concentration time series are characterized by multifractal characteristics. Thus, the threshold level (*Th*) changes the temporal structure of the PM concentration time series. It's demonstrated in this figure at lower *Th* values $\{0, 0.5, 1\}$*WHO-limit and higher *Th* values $\{3.5, 4, 4.5\}$*WHO-limit, that the fractal dimension of PM10 is systematically smaller than PM2.5 ones. Then, at medium *th* values $\{1.5, 2, 2.5, 3\}$*WHO-limit the fractal dimension of PM10 is larger than those of PM2.5. These results suggest that PM10 and PM2.5 concentrations

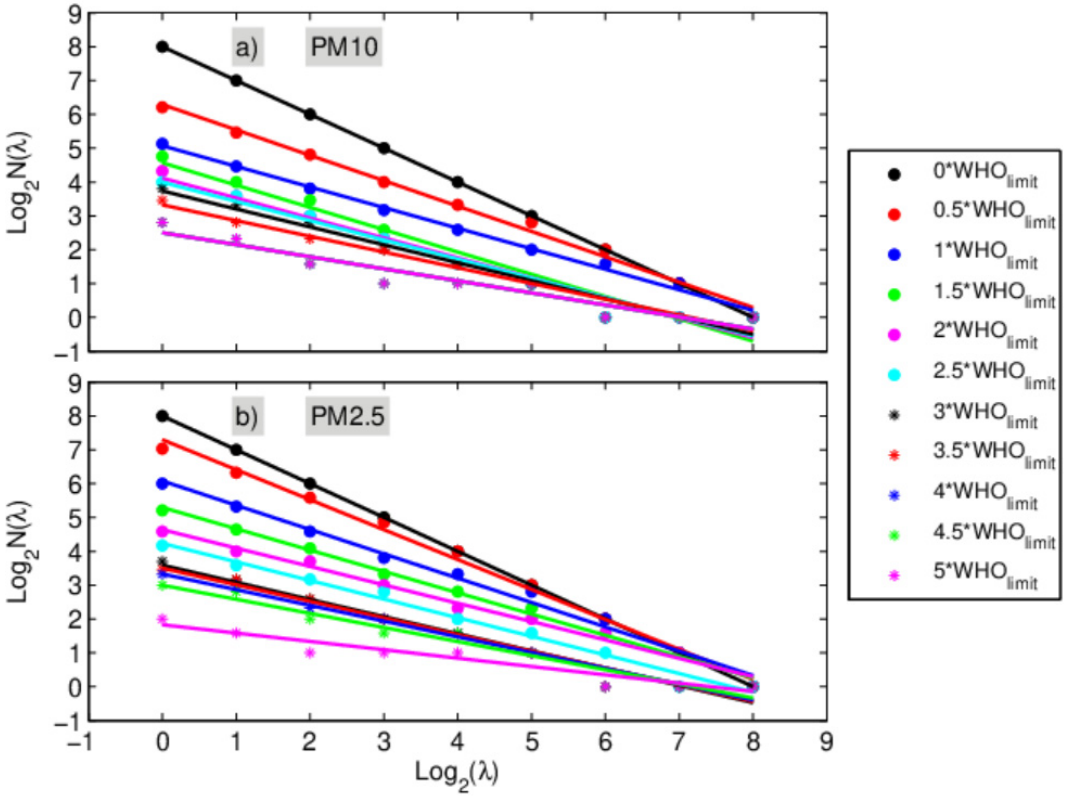

Fig. 5. Box counting graph derived from daily particulate matter concentration: (a) for PM10 measurements; (b) for PM2.5 measurements

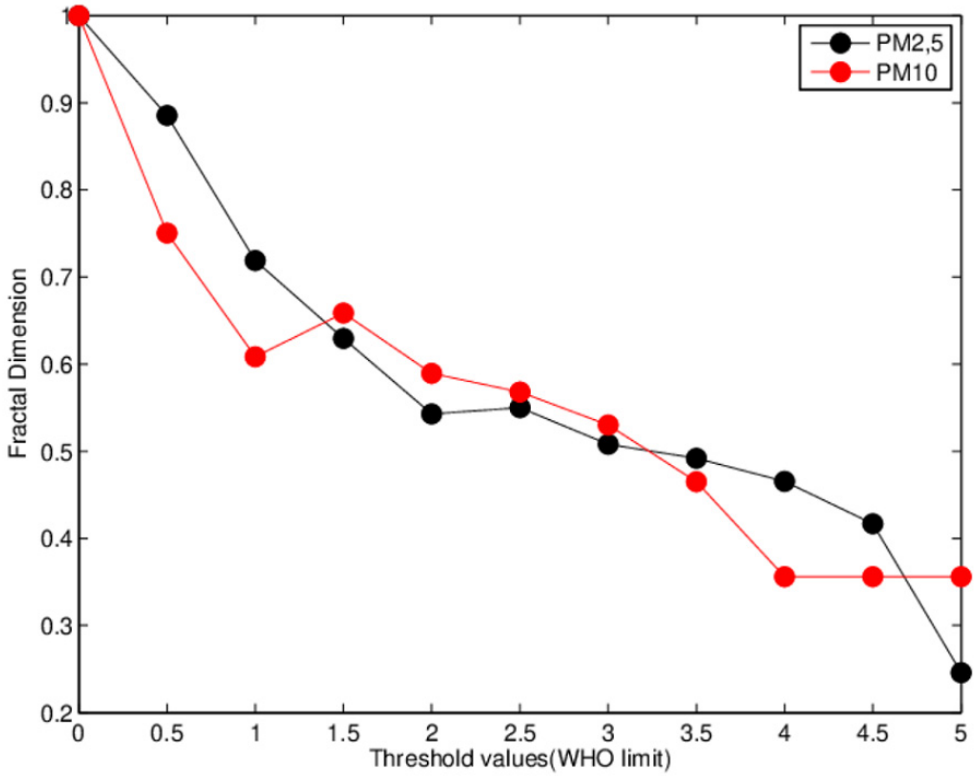

Fig. 6. Fractal dimension (*Df*) versus levels thresholds, *Th*

are provided by different sources. These results suggest that, for lower and higher threshold levels, PM10 concentration time series present high intermittency compared to PM2.5 ones. Opposite results are obtained for the medium threshold level. For higher *Th* values, the intermittency is constant because the fractal dimensions of PM10 are equal to those of PM2.5. These findings indicate that some temporal characteristics can be revealed in PMs time series by analyzing the relationship between fractal dimension *(Df)* and threshold *(Th)*. However, the study of the single fractal dimension cannot permit describing deeply the distribution of PM concentration in its local fluctuations. Therefore, it's necessary to study this temporal series under a multifractal framework. These results have been corroborated by previous studies such as (Ho et al., 2004; Lee et al., 2002, and Lee et al., 2003a) in Asia.

In Figure 7, the main parameters of PM10 and PM2.5 concentration-time series' multifractal spectra are presented. Overall, the $H(q=2)$, asymmetry index (AI), Holder or singularity exponent (α_0), and the multifractal spectrum width ($\Delta\alpha$) values obtained for the PM10 concentration time series are different from those of PM2.5, but they are closer in some months and vary generally in the same manner (Figure 7). This implies that in each month the fluctuation regimes in the PM10 daily concentration time series are different from that of PM2.5. Thus, some differences are presented in each month for both PM concentrations concerning their emissions sources, which present greater changes between the months.

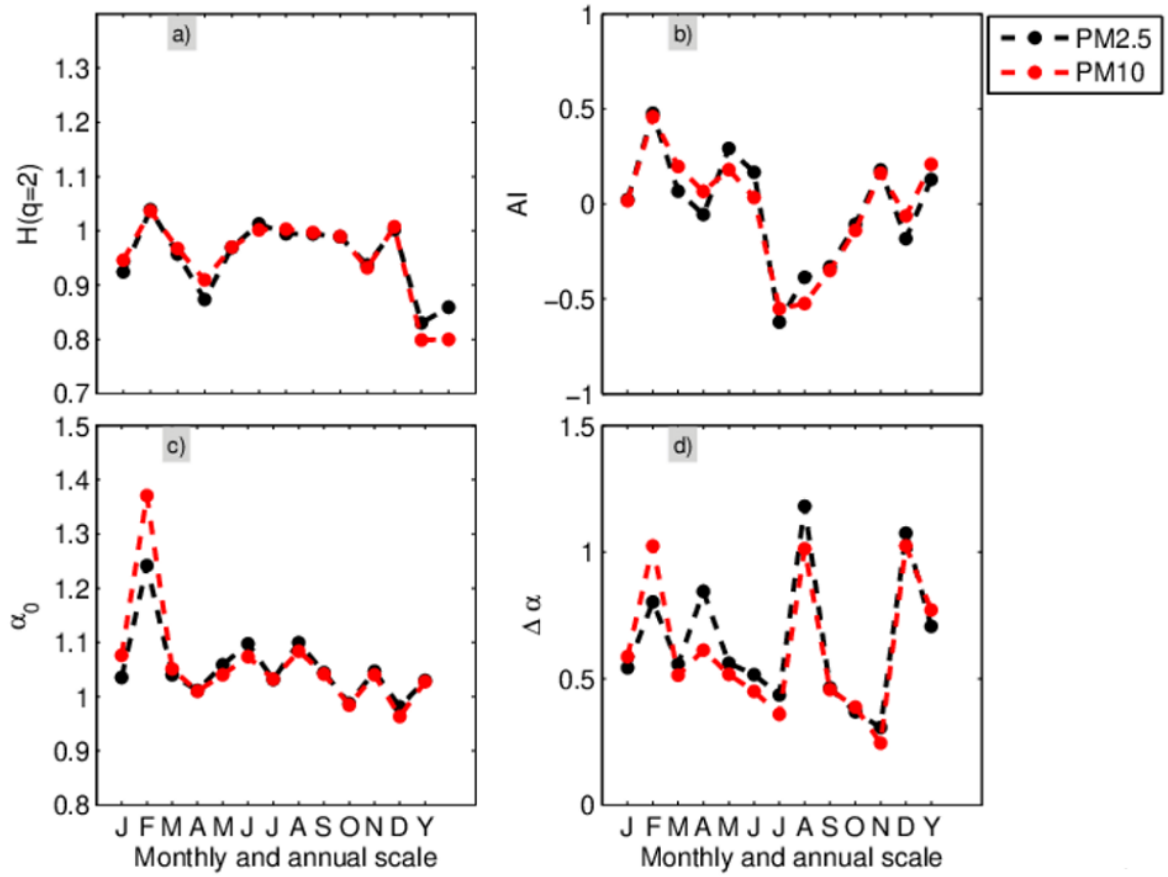

Fig. 7. Hurst exponent and main parameters of monthly and annual multifractal spectra of PM10 (red color) and PM2.5 (black color) concentration time series. For both PM time series, temporal variation of H(q=2), asymmetry index (AI), Holder or singularity exponent (α_o), and the multifractal spectrum width ($\Delta\alpha$) are shown in panels (a), (b), (c), and (d), respectively. January (J), February (F), March (M), April (A), May (M), June (J), July (J), August (A), September (S), October (O), November (N) and December (D), Y stands for Annual scale

It can be observed in Figure 7a the temporal variation of *H(q = 2)*. Except for February and November, *H(q = 2)* values are lower than 1. Therefore, in February and November, the PM10 and PM2.5 concentration time series are non-stationary signals. In February and November, the Hurst exponent, *h (h=H(q=2) -1)* is lower than 0.5, thus in these months, the time series for both PM concentrations are characterized by anti-persistent behavior. They are characterized by persistent behavior during the other months. The results can be interpreted as follows: an increase in the PM10 and PM2.5 daily concentration values is likely to be followed by an increase in PM10 and PM2.5 concentration. These findings are useful in modeling these two examined variables.

The asymmetry index (AI) results obtained each month and annually for PM10 and PM2.5 concentrations time series are presented in Figure 7b. In January, the multifractal spectrum of the daily PM10 and PM2.5 concentrations are symmetric, because AI-value is equal to zero. Therefore, according to Xie and Bao (2004), the singularity of the large and small fluctuations is identical. For PM10 (PM2.5), AI values are negative during July, August, September, and October (April, July, August, September, and October). Therefore, in these months their corresponding multifractal spectrum presents right-hand deviation with local low fluctuations, while the opposite result is obtained during the other months because AI values are positive.

Overall, α_0 varies monthly, however, no trend is obvious (Figure7c). The α_0 values obtained during the month are greater than 1, except during October and December for PM10 and PM2.5 concentration time series (Figure7c). For both PM concentration and among the months examined, February presents the highest value of α_0, while the lowest value is found in December. This result implies that February exhibits the greatest persistence. Generally, except for January, February, and March, the α_0 values of PM2.5 are higher than that of PM10. This finding suggests that in these months PM10 is governed by a more regular process and more variability than PM2.5, whereas the opposite result is obtained in January-February-March.

Overall, for both PMs concentration time series, the multifractal spectrum widths ($\Delta\alpha$) are different from zero during all the months and studied years (Figure 7d). This result confirms the findings obtained above from the box-counting method. Thus, the PM10 and PM2.5 time series may be more suitably described by using a multidimensional fractal structure (or multifractal scaling analysis).

Generally, the multifractal spectra of PM2.5 are wider than that of PM10 during the months of the year, except in January and February, meaning that the fluctuation regimes in PM2.5 are more complex than that of PM10. However, during January, and February, and when the daily time series observed during the studied year are considered, the multifractal spectra of PM10 present a lower width compared to PM2.5. Thus, during these periods, the multifractality degree of PM10 is larger and its time series present more complex behavior. During the studied year and specifically during April, July, September, and October, PM2.5 and PM10 exhibit similar values of multifractal spectra width ($\Delta\alpha$) and therefore present a similar degree of multifractality. Among the studied month, the highest value of ($\Delta\alpha$) is found in February and the lowest value in December. This finding suggests that PM10 and PM2.5 time series are characterized by a larger (smaller) degree of complexity in February (December). This result could be attributed to the nature of its emission sources or an unidentified local process.

According to Xie and He (2019), it's necessary to examine the relationship between PM2.5 and PM10 when studying them around a port area. So, the monthly and annual multifractal spectra of the multifractal detrending moving-average cross-correlation analysis between PM10 and PM2.5 concentration time series are shown in Figure 8. The results have shown that some differences exist between monthly and annual multifractal spectra. Thus, the nonlinear relationship between PM10 and PM2.5 concentration time series changes monthly and the monthly relationship is different from that of the annual scale. It can be observed that the monthly and annual multifractal spectra have a bell-like shape and present a concave-down

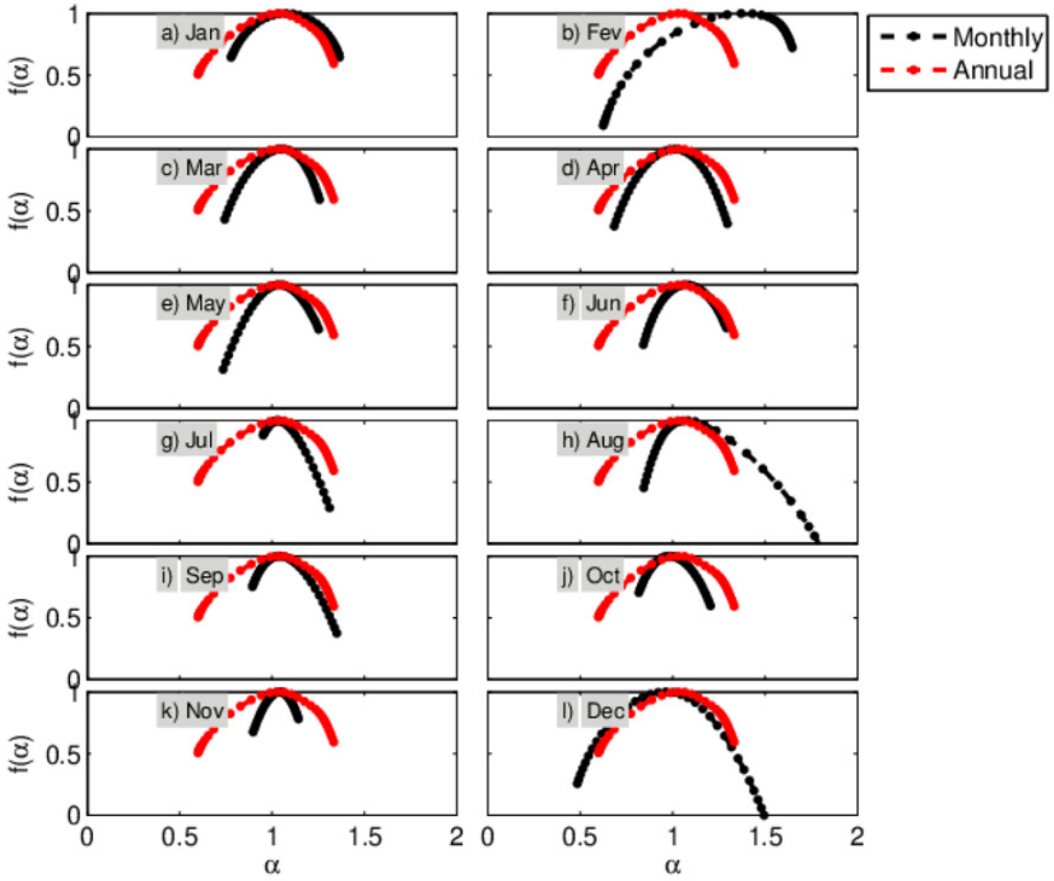

Fig. 8. Monthly (black color) and annual (red color) multifractal spectra obtained from Multifractal detrending moving-average cross-correlation analysis (MFXDMA) between PM10 and PM2.5 concentration time series

parabola. This finding indicates that the cross-correlation between daily PM10 and PM2.5 concentration time series in each month and during the year are multifractal and present strong multifractal characteristics. Thus, the cross-correlation between these PM concentrations is a multiscale series.

Figure 9 presents the Hurst exponent and the main parameters of the monthly and annual multifractal spectra of the multifractal detrending moving-average cross-correlation analysis between PM10 and PM2.5 concentration time series.

As shown in Figure 9a, in all the months of the year, except in February, $h_{xy}(q = 2)$ values are between 0 and 1 and greater than 0.5, meaning positive persistent cross-correlation between PM10 and PM2.5 concentration in these months. Thus, an increase (decrease) in PM2.5 concentrations fluctuations is associated with an increase (or decrease) in PM10 concentrations. The same findings are obtained when one considers all the data observed during the studied year. However, the opposite results are found in February. In this month, an increase (or decrease) in PM2.5 is related to a decrease (or increase) in PM10 concentrations according to the power law. In addition, the persistent behavior of the cross-correlation between PM2.5 and PM10 depends on the month.

As shown in Figure 9b, the asymmetry index (AI) obtained for the cross-correlation multifractal spectra of the cross-correlation between PM10 and PM2.5 is less than zero in July, August, September, October, and December, and the opposite result is obtained in the other months and during the studied year. These findings indicate that the cross-correlation is left-

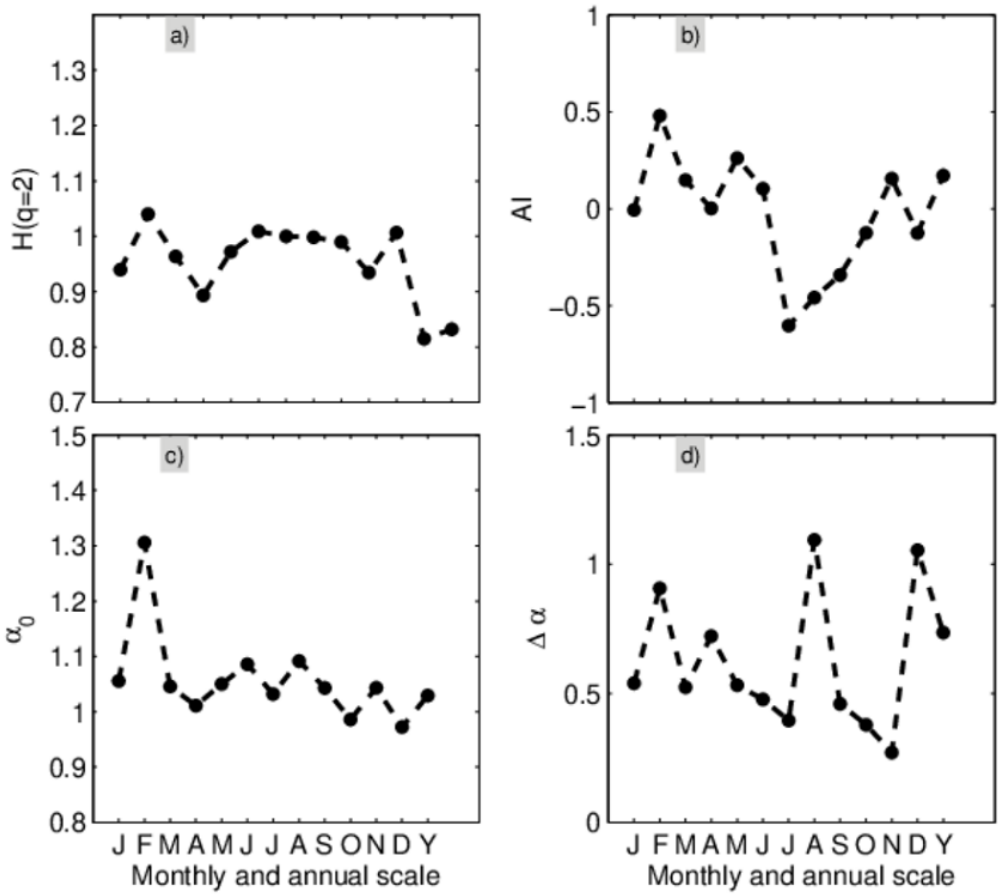

Fig. 9. Main parameters of the monthly and annual multifractal spectra obtained from Multifractal detrending moving-average cross-correlation analysis between PM10 and PM2.5 concentration time series. The temporal variation of *H(q=2)*, asymmetry index (AI), Holder or singularity exponent (α_0), and the multifractal spectrum width (Δα) are shown in panels (a), (b), (c), and (d), respectively. January (J), February (F), March (M), April (A), May (M), June (J), July (J), August (A), September (S), October (O), November (N) and December (D). Y, stands for Annual scale.

skewed in July, August, September, October, and December, and right-skewed in the other months. Thus, low fractal exponents characterize the spectra of the cross-correlation in July, August, September, October, and December.

According to α_0 values (Figure 9c), the multifractality degree of the cross-correlation between PM10 and PM2.5 concentration vary monthly. The cross-correlation between PM2.5 and PM10 presents the highest multifractality in February and the lowest in November.

In the months of the year and during the studied year, the widths (Δα) of the cross-correlation multifractal spectra of the correlation between PM10 and PM2.5 (Figure 9d) are all significantly nonzero. This finding indicates that the cross-correlation between PM10 and PM2.5 presents multifractal nature. In some months named as group1 (January, February, March, April May, August, and December), and during the studied year, the widths are greater than 0.5, thus PM10 and PM2.5 cross-correlation time series present strong multifractality, however, weak multifractality is obtained in others months named as group2 (June, July, September, October, and November). Overall, the temporal fluctuations of the cross-correlation between PM10 and PM2.5 are characterized by greater complexity in group1 than in the group2. Thus, the changes in the temporal fluctuations of the cross-correlation between PM10 and PM2.5 in group1 is larger than in group2.

CONCLUSIONS

The present study aims to provide baseline information in the full understanding of PM2.5 and PM10 concentration time series variations, mainly on the cross-correlation between PM2.5 and PM10 using nonlinear approaches. Daily PM2.5 and PM10 concentration time series measured from January 1st to December 31st, 2020, along the Boulevard de la Marina, a major road in Cotonou are examined by the fractal approach. These data are recorded during the Beninese-German scientific mission financed by the German Corporation for International Cooperation GmbH (GIZ). The box counting method has been used to detect the pollution levels and to analyze the differences in emissions sources for pollution episodes through the fractal dimension. Different threshold levels (Th) or pollution levels are used. The threshold levels are $\{0, 0.5, 1, 1.5, 2, 2.5, 3, 3.5, 4, 4.5\}$*WHO-limit. WHO-limit is the WHO recommendation for the corresponding particulate matter. The multifractal detrending moving-average analysis (MFDMA) is used to analyze the multifractal characteristics of PM2.5 and PM10 concentrations. Multifractal detrending moving-average cross-correlation analysis (MFXDMA) is used to study the cross-correlation between PM2.5 and PM10 concentrations. The most major results can be summarized as follows:

(1) PM10 and PM2.5 concentration time series are characterized by a fractal dimension, which permits to detect the pollution levels and to analyze the differences in emissions sources. For lower $\{0, 0.5, 1\}$*WHO-limit and higher threshold level $\{3.5, 4, 4.5\}$*WHO-limit, PM10 concentration time series present high intermittency compared to PM2.5 ones. Opposite results are obtained for medium threshold level $\{1.5, 2, 2.5 \text{ and } 3\}$* WHO-limit.

(2) Except in February and November, where the opposite results are revealed, daily PM2.5 and PM10 time series observed during the other months and the year are considered. PM2.5 and PM10 are characterized by persistent behavior and are stationary signals.

(3) In all the months of the year, PM2.5 and PM10 fluctuations are characterized by significant multifractal structures, however, the multifractal properties change with the months.

(4) In most of the months, the multifractal degree and complexity of the PM10 time series are characterized by a much stronger multifractal degree and complexity, compared to the PM2.5 time series. However, they present a similar multifractality degree in some months of the year.

(5) The cross-correlation between PM2.5 and PM10 time series in the months of the year is characterized by multifractal characteristics with positive persistence, however, the cross-correlation multifractal features present monthly variation.

The study's findings provide complementary informations for a better understanding of the multiscale dynamics of air pollution, especially providing some reference values for the joint control of the Cotonou port area PM2.5 and PM10 concentrations. This work recommends the use of the practical mathematical tool of Chaos theory to describe PM.25 and PM10 variability, to predict how these variables will behave in the future, and to obtain better short-and long-term forecasts. Moreover, box dimension is recommended here to characterize the temporal structure of (PM2.5, and PM10) concentrations. However, the availability of long-term PM10 and PM2.5 data is needed and strongly recommended to reinforce our conclusions. Future work should address to the cross-correlation analysis between meteorological factors and particulate matter (PM2.5, and PM10) based on multifractal theory. The present study limitations refer to the short study period, which is only one year of available data.

ACKNOWLEDGEMENT

This Beninese-German mission was financed by the German Corporation for International Cooperation GmbH (GIZ) and the authors gladly acknowledge Helga Fink for her support and

the German Ambassador Achim Tröster for authorizing us to install the particle separator system on the roof of his residence. They also gratefully thank Aron Kneer and Selçuk Yurtsever-Kneer for the organization of the mission on the German side and their endless efforts to enhance academic education and research in Cotonou. The authors are very grateful to the anonymous reviewers for their valuable comments and constructive suggestions, which helped us to improve the quality of the paper substantially.

GRANT SUPPORT DETAILS

This study received no other funding support.

DATA AVAILABILITY

The PMs concentrations data used in this study are not available online in any database so we cannot provide a link to reach them. However, the datasets are available from the German Corporation for International Cooperation GmbH (GIZ) upon reasonable request.

CONFLICT OF INTEREST

The authors declare that there is not any conflict of interests regarding the publication of the manuscript. In addition, the ethical issues, including plagiarism, informed consent, misconduct, data fabrication and/or falsification, double publication and/or submission, and redundancy has been completely observed by the authors.

LIFE SCIENCE REPORTING

No life science threat was practiced in this research.

REFERENCES

Agbazo, M.N., Koto N'Gobi, G., Alamou, E., Kounouhewa, B. and Afouda, A. (2021). Assessing Nonlinear Dynamics and Trends in Precipitation by Ensemble Empirical Mode Decomposition (EEMD) and Fractal Approach in Benin Republic (West Africa). Hindawi, Complexity, vol. 2021, Article ID 3689397, 14 pages. https://doi.org/10.1155/2021/3689397.

Agbazo, M.N., Koto N'Gobi, G., Alamou, E., Kounouhewa, B. and Afouda, A. (2019). Fractal analysis of the long-term memory in precipitation over Benin (West Africa). Advances in Meteorology, vol. 2019, no. 2, pp. 1-12.

Arianos, S. and Carbone, A. (2007). Detrending moving average algorithm: a closed-form approximation of the scaling law. Physica A 382, 9-15.

Awokola, B. I., Okello, G., Mortimer, K.J., Jewell, C.P., Erhart, A. and Semple, S. (2020)
Measuring air quality for advocacy in Africa (MA3): Feasibility and practicality of longitudinal ambient PM2.5 measurement using low-cost sensors. International journal of environmental research and public health, 17(19), 7243.

Biaou, A. (2004). De la méso-échelle à la micro-échelle: désagrégation spatio-temporelle
multifractale des précipitations. Thèse de l'Ecole des Mines de Paris, Paris, France.

Dossou, K.M.and Glehouenou-Dossou, B. (2007). The vulnerability to climate change of Cotonou (Benin) rising in sea level. Environ. Urban, 19, 65-79.

Djossou, J., Léon, J.F., Akpo, A.B., Liousse, C., Yoboué, V., Bedou, M. and Awanou, C.N. (2018). Mass concentration, optical depth and carbon composition of particulate matter in the major southern west African cities of Cotonou (Benin) and Abidjan (Côte d'Ivoire). Atmospheric Chemistry and Physics, 18(9), 6275-6291

Esposito, E., De Vito, S., Salvato, M., Bright, V., Jones, R.L. and Popoola, O. (2016). Dynamic neural

network architectures for on-field stochastic calibration of indicative Low-cost air quality sensing systems. Sensors and Actuators B. Chemical, 231, 701-713.
Evans, M.J., Knippertz, P., Akpo, A., Allan, R.P., Amekudzi, L., Brooks, B., Chiu, J.C., Coe, H., Fink, A.H., Flamant, C., Jegede, O.O., Leal-Liousse, C., Lohou, F., Kalthoff, N., Mari, C., Marsham, J.H., Yoboué, V. and Reimann-Zumsprekel, C. (2018). Policy-relevant findings of the Dacciwa project, doi: 10.5281/zenodo.1476843.
Feder, J. (1988). Fractals. Plenum Press, New York.
Gao, X., Wang, X. and Shi, H. (2019). Multifractal cascade analysis on the nature of air pollutants concentration time series over China. Aerosol and Air Quality. Research, 19(9), 2100-2114.
Gu, G.F. and Zhou, W.X. (2010). Detrending moving average algorithm for multifractals. Phys. Rev. E 82.
Hubert, P. and Carbonnel, J.P. (1989). Dimensions fractales de l'occurrence de pluie en climat soudano-sahélien. Hydrologie Continentale. 4(1) : 3-10.
Ho, D.S., Juang, L.C., Liao, Y.Y., Wang, C.C., Lee, C.K., Hsu, T.C. and Yu, C.C. (2004). The temporal variations of PM10 concentration in Taipei: a fractal approach. Aerosol and Air Quality Research 4(1), 38-55.
Jiang, Z.Q. and Zhou, W.X. (2011). Multifractal detrending moving average cross-correlation analysis. Phys. Rev. E 84, 016106.
Kounouhewa, B., Koto N'Gobi, G., Houngue, H., Müller, L., Wirtz, M., Yurtsever-Kneer, S. and Barbe, S. (2020). Cotonou's next breath: Particulate matter monitoring and Capturing. Scientific African, 8, e00367.
Kinney, P.L. (2008). Climate change, air quality, and human health. American journal of preventive medicine. 35(5), 459-467.
Knippertz, P., Coe, H., Chiu, J.C., Evans, M.J., Fink, A. H., Kalthoff, N. and Marsham, J.H. (2015). The DACCIWA project: Dynamics-aerosol-chemistry-cloud interactions in West Africa. Bulletin of the American Meteorological Society, 96(9), 1451-1460.
Liu, Z., Wang, L. and Zhu, H. (2015). A time–scaling property of air pollution indices: a case study of Shanghai. China. Atmospheric Pollution Research, 6(5), 886-892.
Lee, C. K. (2002). Multifractal characteristics in air pollutant concentration time series. Water Air Soil Pollut. 135, 389–409. https://doi.org/10.1023/A:1014768632318.
Lee, C.K., Ho, D.S., Yu, C.C. and Wang, C.C. (2003a). Fractal analysis of temporal variation of air pollutant concentration by box counting. Environ. Modell. Software 18, 243–251. https://doi.org/10.1016/S1364-8152(02)00078-6.
Lee, C.K., Ho, D.S., Yu, C.C., Wang, C.C. and Hsiao, Y. H. (2003b). Simple multifractal cascade model for air pollutant concentration (APC) time series. Environmetrics 14, 255-269. https://doi.org/10.1002/env.584.
Liu, L., Huang, G.H, Liu, Y., Fuller, G.A. and Zeng, G.M. (2003). A fuzzy-stochastic robust programming model for regional air quality management under uncertainty. Engineering Optimization, 35(2), 177-199.
Lovejoy, S., Schertzer, D. and Tsonis, A. A. (1987). Functional Box-counting and Multiple Elliptical Dimensions of Rain. Science, 235: 1036-1038.
Mandelbrot, B. (1982). The fractal geometry of nature. San Francisco: W. H. Freeman.
Makowiec, D. and Fulinski, A. (2010). Multifractal detrended fluctuation analysis as the estimator of long-range dependence. Acta Physica Polonica, vol. 41, pp. 1025-1050.
Mama, D.D., Biaou, A., Adounkpe, M., Ahomadegbe, J., Youssao, M., Kouazounde, A. and Kouanda, J. (2013). Transport urbain au (Benin) et pollution atmosphérique : Evaluation quantitative de certains polluants chimiques de (Cotonou). International Journal of Biological and Chemical Sciences, 7(1), 377-386.
Mayer, H. (1999). Air pollution in cities. Atmospheric Environment, 33(24-25), 4029-4037.
Movahed, M.S., Jafari, G.R., Ghasemi, F., Rahvar, S., Tabar, M.R.R. (2006). Multifractal detrended fluctuation analysis of sunspot time series. J. Stat. Mech. Theory Exp., P02003-P02003.
Nikolopoulos, D. Moustris, K. Petraki, E., Koulougliotis, D. and Cantzos, D. (2019). Fractal and long-memory traces in PM10 time series in Athens, Greece Environments, 6(3), 29.
Nikolopoulos, D. Moustris, K., Petraki, E. and Cantzos, D. (2021). Long-memory traces in PM10 time series in Athens, Greece: investigation through DFA and R/S analysis. Meteorology and Atmospheric Physics, 133(2), 261-279.

Nikolopoulos, D., Alam, A., Petraki, E., Papoutsidakis, M., Yannakopoulos, P. and Moustris, K. (2021). Stochastic and Self-Organisation Patterns in a 17-Year PM10 Time Series in Athens, Greece. Entropy 2021, 23, 307. https://doi.org/10.3390/e23030307.

Peitgen, H. O., Jurgens, H.and Saupe, D. (2004). Chaos and Fractals. Springer, Berlin.

Shi, K., Liu, C. and Huang, Y. (2015). Multifractal processes and self-organized Criticality of PM2. 5 during a typical haze period in Chengdu, China. Aerosol and Air Quality Research, 15(3), 926-934.

Shi, K., Liu, C. Q., Ai, N. S. and Zhang, X. H. (2008). Using three methods to investigate time-scaling properties in air pollution indexes time series. Nonlinear Anal. Real World Appl., 9, 693–707.

Shi, K. Liu, C. Q. and Ai, N. S. (2009). Monofractal and multifractal approaches in investigating temporal variation of air pollution indexes. Fractals, 17(04), 513-521.

Wang, L., Zhang, H., Mao, L., Li, S. and Wu, H. (2020). Assessing Spatiotemporal Characteristics of Urban PM2.5, Using Fractal Dimensions and Wavelet Analysis. Mathematical Problems in Engineering, 15 pages. https://doi.org/10.1155/2020/8091515.

World Health Organization (2016). Ambient air pollution: A global assessment of exposure and burden of disease. Working Papers, World Health Organization.

World Health Organization (2018). How Air Pollution is Destroying Our Health. Available online: https://www.who.int/air-pollution/news-and-events/how-air-pollution-is-destroying-our-health.

World Health Organization (2020). Ambient Air Pollution, Global Health Observatory (GHO) data. Available online. https://www.who.int/gho/phe/outdoor-air-pollution/en.

Xepapadeas, A. (1992). Optimal taxes for pollution regulation: Dynamic, spatial and stochastic characteristics. Natural Resource Modeling, 6(2), 139-170.

Xie, S. and Bao, Z. (2004). Fractal and multifractal properties of geochemical fields. Mathematical Geology, vol. 36, no. 7, pp. 847–864.

Xie, H. and He, H. (2019). Multifractal Property Between PM2.5 and PM10 in Hongkong Port. Journal of Atmospheric and Environmental Optics.

Xue, Y., Pan, W., Lu, W. Z. and He, H. D. (2015). Multifractal nature of particulate matters (PMs) in Hong Kong urban air. Science of the Total Environment,532, 744-751.

Xu, L. Ivanov, P.C., Hu, K., Chen, Z., Carbone A. and Stanley, H.E. (2005). Quantifying Signals with power-law correlations: a comparative study of detrended fluctuation analysis and detrended moving average techniques. Phys. Rev. E 71- 051101.

Xu, H.C., Gu, G.F. and Zhou, W. X. (2017). Direct determination approach for the multifractal detrending moving average analysis. Phys. Rev. E 96-052201.

Zhang, C., Ni, Z., Ni, L., Li, J. and Zhou, L. (2016). Asymmetrical multifractal detrending moving average analysis in time series of PM2.5 concentration. Physica A 457, 322-330. https://doi.org/10.1016/j.physa.2016.03.072.

Zhang, C. Wang, X., Chen, S., Zou, L., Zhang, X. and Tang, C. (2019). A study of daily PM2.5 concentrations in Hong Kong using the EMD-based MFDFA method. Physica A 530, 121182. https://doi.org/10.1016/j.physa.2019.121182.

Zhao, D., Chen, H., Yu, E. and Luo T. (2019). PM2.5/PM10 Ratios in Eight Economic Regions and Their Relationship with Meteorology in China. Hindawi, Advances in Meteorology, vol, 2019,15 pages, https://doi.org/10.1155/2019/5295726.

Zhou, W. X. (2008). Multifractal detrended cross-correlation analysis for two non-stationary signals. Phys. Rev. E 77, 066211.